

1 Layering genetic circuits to build a single cell, bacterial half adder

2 Adison Wong^{1,2,†}, Huijuan Wang¹, Chueh Loo Poh^{1*} and Richard I Kitney^{2*}

3
4 ¹School of Chemical and Biomedical Engineering, Nanyang Technological University, Singapore 637459, SG

5 ²Department of Bioengineering, Imperial College London, London SW7 2AZ, UK

6
7 * To whom correspondence should be addressed: Chueh Loo Poh, Division of Bioengineering, School of
8 Chemical and Biomedical Engineering, Nanyang Technological University, Singapore 637459, SG. Tel: +65
9 6514 1088; Email: clpoh@ntu.edu.sg

10
11 * Correspondence may also be addressed to: Richard Ian Kitney, Centre for Synthetic Biology and Innovation,
12 and Department of Bioengineering, Imperial College London, London SW7 2AZ, UK. Tel: +44 (0)20 7594 6226;
13 Email: r.kitney@imperial.ac.uk

14
15 †Present Address: NUS Synthetic Biology for Clinical and Technological Innovation, National University of
16 Singapore, Singapore 117456, SG

18 ABSTRACT

19 Gene regulation in biological systems is impacted by the cellular and genetic context-dependent
20 effects of the biological parts which comprise the circuit. Here, we have sought to elucidate the
21 limitations of engineering biology from an architectural point of view, with the aim of compiling a set of
22 engineering solutions for overcoming failure modes during the development of complex, synthetic
23 genetic circuits. Using a synthetic biology approach that is supported by computational modelling and
24 rigorous characterisation, AND, OR and NOT biological logic gates were layered in both parallel and
25 serial arrangements to generate a repertoire of Boolean operations that include NIMPLY, XOR, half
26 adder and half subtractor logics in single cell. Subsequent evaluation of these near-digital biological
27 systems revealed critical design pitfalls that triggered genetic context dependent effects, including 5'
28 UTR interference and uncontrolled switch-on behaviour of σ_{54} promoter. Importantly, this work
29 provides a representative case study to the debugging of genetic context dependent effects through
30 principles elucidated herein, thereby providing a rational design framework to program single
31 prokaryotic cell with diversified digital operations.

32 INTRODUCTION

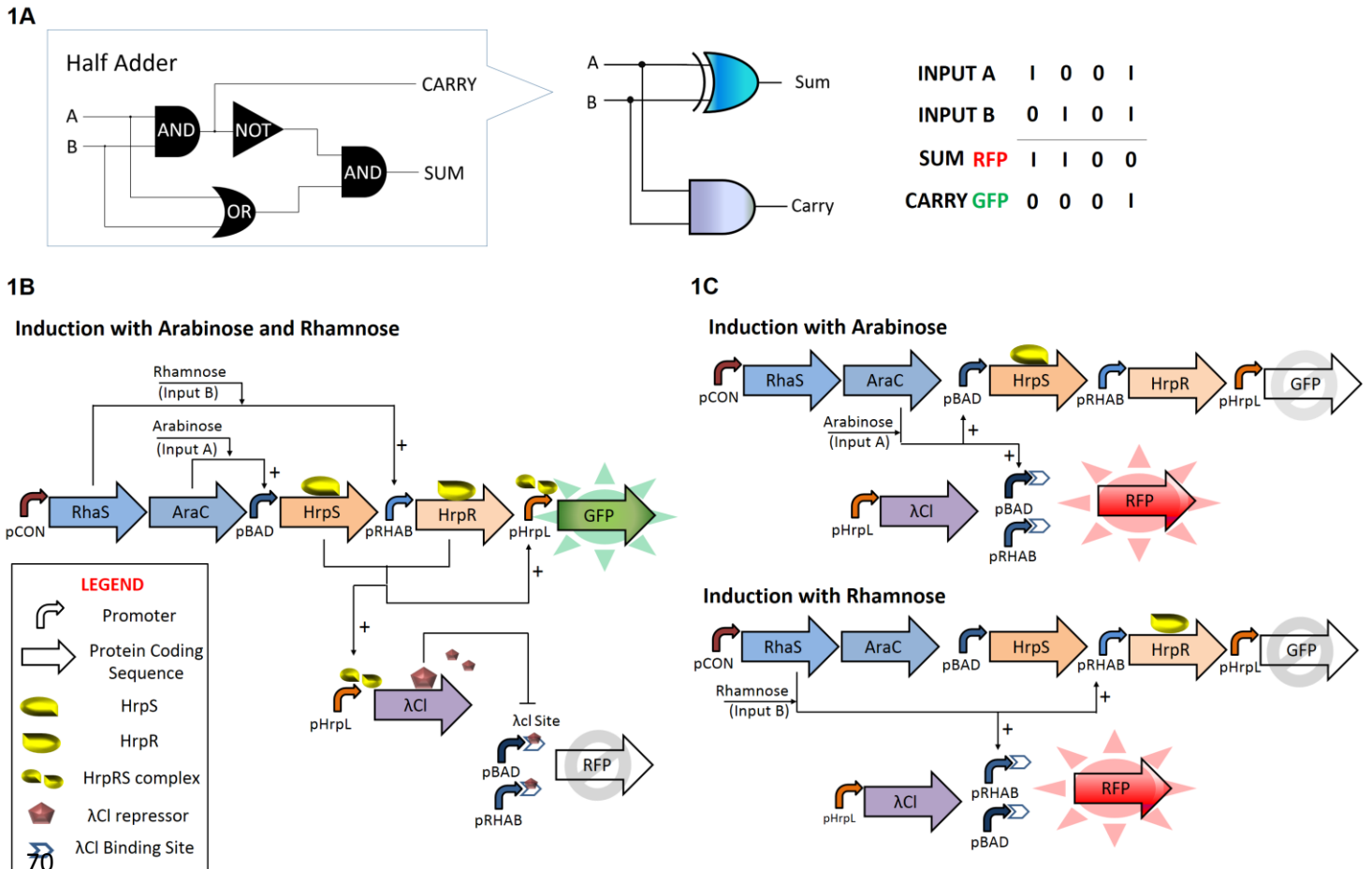
33 Gene regulation in biological systems behaves like molecular computers whereby the gene's output
34 can be modelled as on-off states of Boolean (digital) logic [1-3]. However, programming gene
35 regulation is far from trivial and requires considerable time and effort during functional testing and
36 tuning of the synthetic genetic circuits under development. Apart from the scarcity of reliable and well
37 characterised biological parts, digital performance in biological systems is further impacted by the
38 cellular and genetic context dependent effects of the biological parts which comprise the circuit [4-6].
39 Recent studies have shown that genetic cross-talks between the engineered circuits and endogenous
40 networks of host cell can lead to cellular context dependent effects [7, 8]. For this reason, molecular
41 parts and devices that are orthogonal to the cell native machineries with roles in either genetic
42 transcription or protein translation have been created to enable predictable engineering of genetic

43 circuits [9-13]. Demonstrations of layered genetic circuits in single cell, such as the execution of 4-
44 input AND gate in bacteria [10] and biological half adder and half subtractor in mammalian cells [14]
45 have revealed that orthogonal logic gates can be interlinked to perform digital operations of higher
46 complexity and diversified outputs. While the capability to program cells with memory and decision
47 making functions [15-19] presents many opportunities in biotechnological applications, a lack of
48 formal understanding associated with genetic context dependent effects has limited progress in
49 engineering biology. In this respect, two studies have shown that the 5' untranslated region (5'-UTR)
50 of mRNA can affect the temporal control of multigene operons or inverter-based genetic circuits, and
51 RNA processing using CRISPR or ribozyme can serve as effective genetic insulators to buffer such
52 context dependent effects [5, 20]. In this paper, we have sought to elucidate the limitations of
53 engineering biology from an architecture point of view, with the aim of creating a set of engineering
54 solutions for overcoming failure modes during the development of complex, synthetic genetic circuits.

55 **Design of Biological Half Adder**

56 In this study we were interested in developing biological half adder in prokaryotic systems, particularly
57 in microbes which exhibit much faster cell division and shorter cycle time – so that they can be
58 broadly applied in different biotechnological applications. In contrast to the mammalian cell-based half
59 adder, which is developed mainly for therapeutic and biosensing applications, a prokaryotic half adder
60 can be used to enhance molecular process control and decision-making – for example in drug and
61 biofuel production, biosensing, bioremediation [21], and probiotic engineering for the treatment of
62 metabolic disorders [22], cancer [23] and infectious diseases [24, 25]. In digital processing half adders
63 form the key building blocks for shift registers, binary counters and serial parallel data converters.
64 Likewise in biological systems, a combination of half adders can be connected in various
65 arrangements to regulate gene expression with diverse, digital-like performance. In doing so,
66 biological systems can be made to interface with novel biomolecular devices, allowing the
67 repurposing of cellular phenotype, as well as providing new platforms to probe and elucidate
68 biological functions [26-28].

69



71 Fig. 1. Simplified schematics of the biological half adder, comprising independent modules of the AND, OR and NOT gates
 72 layered in series and in parallel.
 73 A. Logic output of biological half adder.
 74 B. In the presence of two inputs, the AND gate is activated to produce GFP and lambda repressors, which further
 75 inactivates the OR gate to suppress RFP expression.
 76 C. In the presence of either inputs singly, only the OR gate is activated to trigger RFP expression.

77

78 *Escherichia coli* was chosen as the designated chassis as it represents a model organism that can
 79 be easily manipulated - its inherent cellular processes are also well characterised. Fig. 1 shows the
 80 design of our biological half adder in a single prokaryotic cell. The half adder consists of 3
 81 independent biologically-derived AND, OR and NOT logic gates - and a fourth AND logic function that
 82 is not a physical device, but a result of programmable decision making as a result of interconnecting
 83 logic functions (Fig. 1A). The σ^{54} -dependent HrpRS regulation motif of *Pseudomonas syringae* T3SS
 84 secretion system was refactored for the design of the AND gate, as demonstrated in an earlier study
 85 [12]. The advantage is that the HrpRS AND gate offers dual layer of orthogonal control in *E. coli* host.
 86 This means that (a) the majority of transcription events in *E. coli* occurs via σ^{70} -dependent
 87 transcription, and (b) HrpRS transcription factors are absent in wild type *E. coli*. Transcription occurs
 88 when enhancer-binding proteins HrpS and HrpR, which are regulated by arabinose (input A) and
 89 rhamnose (input B) induction respectively, are coexpressed and bound to the upstream activator sites

90 of pHrpL promoter. This binding event then triggers an ATPase-dependent conformational change
91 within the promoter through a molecular interplay with the σ^{54} -RNAP holoenzyme, thereby allowing
92 RNA synthesis and elongation after the transcription start site. The OR gate generates mRNA
93 transcript of the RFP gene upon induction with either arabinose or rhamnose. The NOT gate in the
94 half adder design is a hybrid promoter consisting of λ CI repressor binding sites downstream of the
95 transcriptional start site (TSS) of OR logic gate. Unlike traditional NOT gates, which are designed to
96 have transcriptional repressors competing for consensus RNAP binding sites, our NOT gate design
97 functions as an orthogonal, molecular blocker to the RNA elongation process.

98 On induction with arabinose and rhamnose, the transcription factors AraC and RhaS, both of which
99 are constitutively expressed in a single transcript by promoter pCON, associate with their
100 corresponding inducers to activate expression of the enhancer-binding proteins HrpS and HrpR. This
101 results in the activation of the AND logic and the concurrent synthesis of GFP reporter and lambda
102 repressor (λ CI) by the pHrpL promoter. Consequently, genetic events of the OR gate, which run in
103 parallel with the HrpRS AND gate, is then turned off due to obstructive repression by λ CI molecules.
104 In all, the half adder demonstrates both AND (SUM Output) and XOR (CARRY Output) logic
105 operations, the latter operation is a processed outcome achieved by sequential and parallel layering
106 of AND, OR and NOT logic (Fig. 1B). By comparison, induction with either inducer singly will trigger
107 only genetic operation of the OR gate, resulting in the synthesis of RFP reporter, but not GFP and λ CI
108 molecules (Fig. 1C). Finally, we also demonstrate the development of a single cell prokaryotic, half
109 subtractor via slight modifications to the half adder circuit.

110 MATERIAL AND METHODS

111 Strains, plasmids and growth conditions

112 *E. coli* strain Top10 (Invitrogen) was used for all the cloning and characterisation experiments. The
113 genes and oligonucleotides used in this study were synthesized by either Geneart (Life Technologies,
114 Grand Island, NY) or Sigma Aldrich (St. Louis, MO). All the enzymes used in this study, including
115 OneTaq and Phusion polymerase, T4 ligase, EcoRI, XbaI, SpeI, PstI and DpnI, were obtained from
116 New England Biolabs. Chloramphenicol ($35\mu\text{gml}^{-1}$) and ampicillin ($100\mu\text{gml}^{-1}$) were added to culture
117 media for experiments involving pSB1C3 and pSB4A5 plasmid vectors, where appropriate. In all the
118 characterisation experiments, cells were inoculated from freshly transformed plates were grown in 2ml
119 LB (Miller, BD Bioscience, San Jose, CA) with appropriate antibiotic in 50ml Falcon tubes overnight at
120 37°C with 225rpm shaking unless otherwise stated. Overnight cultures were then diluted to $\text{OD}_{600} \sim$
121 0.002 in 5ml LB antibiotic and further grown to a final OD of 0.5 ± 0.05 with the same culture
122 conditions (37°C and 225rpm shaking). Harvested cells were kept on ice until induction. All inducers
123 used in this study were purchased from Sigma Aldrich with final concentration ranging from 0 to
124 28mM.

125 System assembly

126 All genes from *E. coli* (*pBAD*, *pRHAB*, *araC* and *rhaS*) were cloned from genomic DNA of strain
127 MG1655 (ATCC 700926). *hrpS*, *hrpR* and *pHrpL* were cloned from an earlier study [12] while *pCON*
128 (Bba_J23101), double terminator (Bba_B0015), GFPmut3b (Bba_E0040), RFP (Bba_E1010) and λ Ci
129 (Bba_C0051) were cloned from the BioBrick registry. PCR was performed using Phusion DNA
130 polymerase in a dual cycle PCR programme at annealing temperatures of 53°C and 60°C for the first
131 7 and subsequent 20 cycles, respectively. Biological parts were spliced by overlap extension PCR
132 and ligated to vectors pSB4A5 (low copy, pSC101 replication origin) and pSB1C3 (high copy, pMB1
133 replication origin) using XbaI and PstI restriction sites. Composite systems with two or more biological
134 modules were sequentially assembled as previously described [25].

135 **Parts mutation of λ Ci repressor binding sites**

136 To obtain sequence variants of λ Ci repressor binding sites, PCR with randomised primers and
137 Phusion DNA polymerase were performed on pHrpL- λ Ci-pBAD-Ci2A template with primers 5'-
138 ttcgaattcgcggccgcttctagaggccgattat and 5'-gctactagtatatNNNNNNNNccggtgatatatggagaaacagta
139 (restriction sites underlined). The resultant amplifcons (~1.4kb) were then ligated upstream to
140 pSB1C3 vector containing an RFP reporter and transformed to competent cells carrying HrpRS AND
141 gate modules in pSB4A5. Single colonies of uniform size were inoculated into 96 well microplate
142 loaded with 200ul LBAC (LB with chloramphenicol and ampicillin) and grown in microplate incubator
143 set at 37°C with 750rpm shaking for 6 hours. Accordingly, cultures in each well were triplicated and
144 diluted 10x into 200ul LBAC with 3.5mM arabinose and 28mM rhamnose, 3.5mM arabinose, and no
145 arabinose in the same growth condition. Evolved mutants were identified by observable differences in
146 RFP expression and inhibition after 6 hours of induction using Fluostar OPTIMA microplate reader
147 (BMG Labtechnologies). Validation and characterisation of isolated candidate parts was
148 independently performed in 175ul LBAC in 1.5ml microcentrifuge tubes after 4 hours induction at 37°C
149 and 1000rpm shaking under four different logic conditions.

150 **Modelling of AND, OR and NIMPLY logic gates**

151 To enable model-driven design synthetic biological systems, we examine the effect of ribosome
152 binding sites (RBS) on the steady state transfer function of input switch devices. By analysing
153 reference data [12] that had previously characterise the input-output relationship of genetic switches
154 in the form of Eqn. 1, we observed that parameters that are most sensitive to changes in RBS are
155 parameters A and B. Hence, by knowing the relative output of switch devices with weaker RBS by
156 either prediction from reliable software or by single experimental measurement of device's output at
157 input maximal, the parameters A and B can be scaled proportionally to obtain *a priori* parameters that
158 accurately predict the transfer function of other devices with weaker RBS (Supplementary Fig. 1A).
159 We validated our approach with previously published data sets (Supplementary Table 1) and showed
160 that the transfer function of input devices pLuxR (Supplementary Fig. 1B) and pBAD (Supplementary
161 Fig. 1C) with different RBS can be reliably estimated without additional experimentation. MatLab
162 modelling scripts are available in Supplementary Material II.

163 The transfer functions of input switch devices used in this work with strong RBS were empirically
164 fitted into the Hill-like equation (Eqn. 1), while those of input switch devices with weak RBS were
165 predicted using the validated method as discussed above. Supplementary Table 3 shows the
166 empirical transfer function parameters of the various input switch devices. AND and OR gate profiles
167 were then modelled and predicted using these parameters and equations as shown in Supplementary
168 Materials Eqn. 7 and 10. Supplementary Fig. 11, 12 and 13 show the predicted normalised output of
169 the HrpRS AND gate and various OR gates combination. NIMPLY gate was empirically modelled
170 using Supplementary Materials Eqn. 2 and parameters from Supplementary Table 2. Supplementary
171 Fig. 10 shows the predicted output of NIMPLY gate.

172 **Characterisation and orthogonality testing of input switch devices**

173 To characterise input switch devices, reinoculated cultures at $OD_{600} \sim 0.5$ were transferred to black,
174 flat-bottom 96-well plates (Greiner Bio-One, cat. no. 655090) in aliquots of 150 μ l for induction with
175 rhamnose or arabinose in serial 2 fold dilution with highest inducer concentration at ~ 28 mM (i.e.
176 0.00M, 8.38E-07M, 1.68E-06M, 3.35E-06M, 6.70E-06M, 1.34E-05M, 2.68E-05M, 5.36E-05M, 1.07E-
177 04M, 2.14E-04M, 4.29E-04M, 8.58E-04M, 1.72E-03M, 3.43E-03M, 6.86E-03M 1.37E-02M, 2.75E-
178 02M). Plates were then sealed with gas-permeable foils and incubated at 37°C with 750rpm shaking
179 for 3 hours. Fluorescence and optical density data were collected using Fluostar Optima microplate
180 reader (BMG Labtech.) and zeroed with blank LB media with antibiotic to remove background
181 fluorescence and OD_{600} . All results were normalized with OD_{600} -estimated cell density (validated with
182 viable cell counts) and provided in arbitrary units. In the orthogonal testing of input switch devices, the
183 above procedures were repeated with constructs that contain pRHAB-RFP-pBAD-GFP, with fixed
184 concentration of 0.02% arabinose or rhamnose added as appropriate. The experimental results were
185 fitted using an empirical mathematical model [25] (Hill equation),

$$186 \quad Y = A + \frac{B [X]^n}{C^n + [X]^n} \quad (1)$$

187 Equation 1 models reporter output (Y) as a function of input concentration of inducer ($[X]$). The four
188 parameters (A , B , C , n) were estimated to obtain the best fit curve by performing a nonlinear curve
189 fitting using the experimental results. This curve fitting was performed using the nonlinear least
190 square fitting functions in MATLAB Curve Fitting Toolbox (The Mathworks, Natwick, MA, USA).

191 **Characterisation of AND, OR, NIMPLY, XOR, half adder and half subtractor**

192 To characterise the steady state profile of AND and OR logic devices, reinoculated cultures at OD_{600}
193 ~ 0.5 were transferred to black, flat-bottom 96 well plates (Greiner Bio-One, cat. no. 655090) in
194 aliquots of 150 μ l for induction with varying concentrations of rhamnose and arabinose ranging from
195 8.38E-07M to 2.74E-02M. The plates were sealed with gas-permeable foils and incubated at 37°C
196 with 750rpm shaking for 3 hours. Fluorescence and optical density data were collected using Fluostar
197 Optima microplate reader (BMG Labtech.) and zeroed with blank LB media.

198 To characterise the steady state profile of NIMPLY, XOR, half adder and half subtractor logic
199 devices, the above procedures were repeated with slight modifications to reduce evaporation losses
200 in constructs with weaker RBS-RFP modules. Briefly, reinoculated cultures were dispensed in 175µl
201 aliquots into 1.5ml capped-tubes and induced with varying concentrations of rhamnose and arabinose,
202 as above. The aliquots were incubated on a thermomixer platform (Eppendorf) set at 37°C with
203 1000rpm shaking for 4 hours. 150µl aliquots from each tube were transferred to black, flat-bottom 96
204 well plates and assayed for fluorescence and optical density with Synergy HT or H1m microplate
205 readers (Biotek Instruments Inc.). To assess the digital performance of all logic devices, cell cultures
206 were separately induced with water, 28mM rhamnose or/and 7mM arabinose in four different logic
207 conditions. The induced cultures were incubated in the respective conditions as described above and
208 assayed for fluorescence. All results were normalized with OD₆₀₀-estimated cell density and provided
209 in arbitrary units.

210 **Fluorescence imaging of AND & OR gates**

211 For the acquisition of fluorescent images in AND and OR logic devices, reinoculated cultures were
212 transferred to 50ml tubes in aliquots of 5ml and separately induced with water, 28mM rhamnose
213 or/and 7mM arabinose in four different logic conditions overnight. After 15 hours, cell pellet were
214 harvested and transferred to 1.5ml tubes for fluorescent imaging with suitable filters. Images were
215 acquired with high mega-pixel mobile phone camera.

216 **Flow cytometry**

217 Reinoculated cultures were dispensed in 175µl aliquots into 1.5ml capped-tubes and separately
218 induced with water, 28mM rhamnose or/and 7mM arabinose in four different logic conditions. The
219 aliquots were grown on a thermomixer platform (Eppendorf, Germany) set at 37°C with 1000rpm
220 shaking for 4 hours. Before assay, 5µl culture from each sample were diluted 200x in 0.22µm filtered
221 DI water (pH 7). All expression data were collected using BD LSRFortessa X-20 flow cytometer (BD
222 Biosciences, San Jose, CA) with a 488nm argon excitation laser, and 530nm±30 (FITC) and
223 610nm±20 (PE-CF594) emission filters. The data were gated using both forward (550v, threshold
224 1500v) and side scatter (310v) with the neutral density filter removed. At least 10,000 events were
225 recorded per sample. FITC and PE594 channels were set at 466v and 852v respectively. Data
226 analysis was performed with FlowJo (TreeStar Inc., Ashland, OR).

227 **RESULTS**

228 **Characterisation of Input Devices**

229 The choice of input signals presents the first possible complication in terms of parts modularity. For
230 this reason, genetic circuits of higher complexity with multiple inputs often utilise promoter systems
231 which are activated by inducers of vastly dissimilar chemical nature, namely IPTG, tetracycline,
232 arabinose, 3OC12HSL and C4HSL. Previous studies have shown that a subset of quorum sensing
233 promoters can be activated by homoserine lactone inducers of similar carbon chain length [29, 30].

234 Likewise, wild type pBAD promoter is affected by lactose analogues, requiring further mutagenesis to
235 avoid crosstalk inhibition [31]. Instances of cross-phosphorylation have also been observed in two
236 component signal transduction systems between otherwise distinct pathways [32]. Thus, it is
237 important that inducible input devices are carefully characterised for their steady state transfer
238 function and pairing compatibility before further assembly into higher ordered logic devices.

239 While previous studies with pRHAB promoter involved genetic circuits that include both RhaR and
240 RhaS transcription factors [33-35], in this paper we demonstrate that the rhamnose inducible
241 promoter pRHAB requires only RhaS for full activation and displays tight regulation even when RhaS
242 is overexpressed. Supplementary Fig. 2C and S3C show the steady state transfer functions of input
243 device A, pBAD (Supplementary Fig. 2A) and input device B, pRHAB (Supplementary Fig. 3A)
244 expressing RFP under strong RBS by their corresponding inducers, respectively.

245 To examine the possibility of genetic cross-communication, we constructed genetic circuits that
246 couple GFP production to pBAD activation and RFP production to pRHAB activation. The results
247 show that varying concentration of arabinose did not activate pRHAB promoter activity
248 (Supplementary Fig. 4A). A similar trend was observed in pBAD promoter with rhamnose
249 (Supplementary Fig. 4B). Interestingly, the simultaneous introduction of both sugars modified the
250 transfer function of each promoter slightly, which may be a result of differential cell growth, sugar
251 import rate or antagonistic effect of one sugar to another. This effect, however, is insignificant as
252 definite ON and OFF switch behaviours are apparent - thereby confirming the pairing compatibility of
253 pBAD and pRHAB promoters.

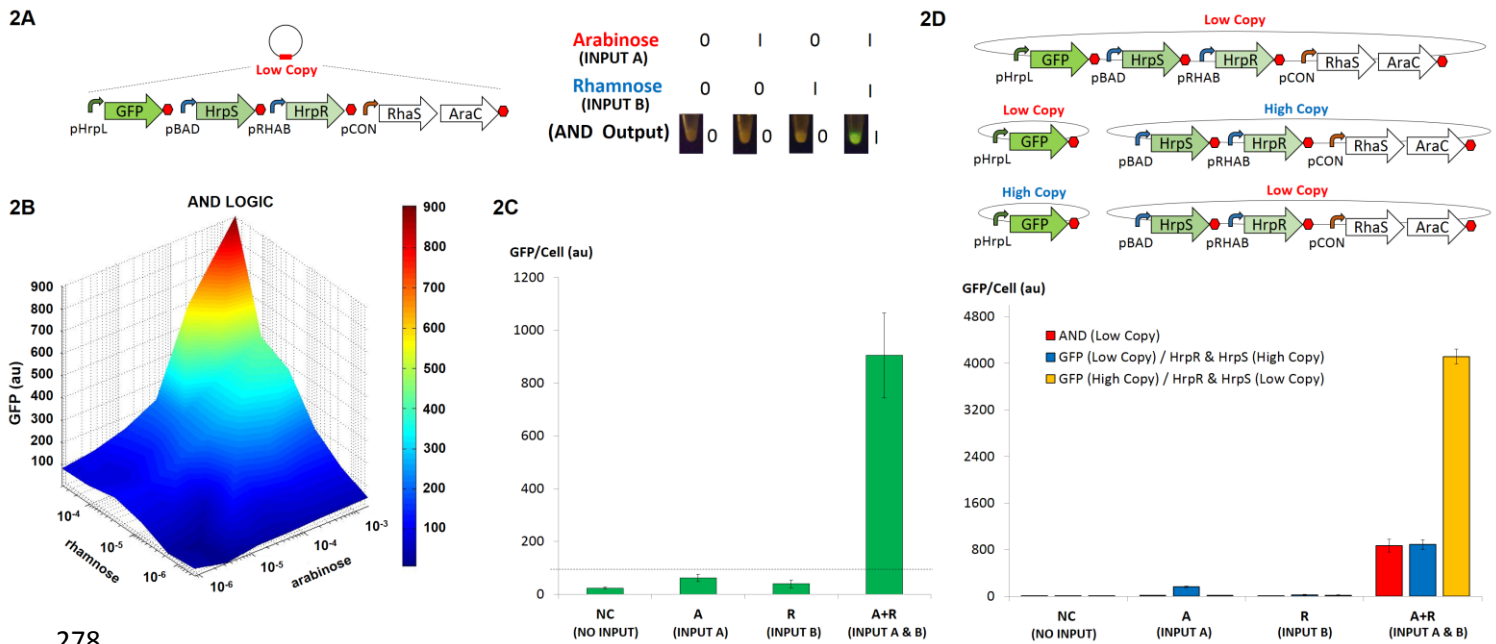
254 **Design and Characterisation of AND Logic Gate**

255 Designs of highly modularised, prokaryotic AND logic devices have hitherto involved the use of
256 multiple plasmids [10, 12, 16, 36, 37]. In this work, we assembled AND logic gate in a single plasmid.
257 This procedure has enabled us to localise AND logic gate in a single vector, and facilitated the
258 downstream troubleshooting and tuning of layered genetic circuits.

259 To develop the AND logic component of the half adder, we systematically designed and
260 assembled refactored modules of the HrpRS transcription machinery into a low copy plasmid (Fig.
261 S2A). The module which expressed GFP from pHrpL promoter was assembled upstream of pBAD-
262 HrpS and pRHAB-HrpR modules to attenuate genetic context dependent effects that might arise from
263 transcriptional overrun of the stronger pBAD and pRHAB input expression modules as a result of
264 inefficient transcription termination. While designing the GFP producing module in a bidirectional
265 permutation is usually a better solution, this option was not tested in our study as the downstream
266 pBAD promoter is a weak constitutive promoter in the reverse complement direction. Thus, placing
267 the pHrpL-GFP module before pBAD in either the reverse or reverse complement arrangement may
268 result in antisense-GFP interference or the occurrence of leaky AND gate. The steady state profile of
269 the functional AND gate was characterised by titrating with a varying concentration of arabinose (input
270 A) and rhamnose (input B) as shown in Fig. 2B. Results of the engineered AND gate correlated well

271 with our steady state computational model (Supplementary Fig. 11), which was applied to match
 272 biological modules making up the AND gate. Likewise, the “on” and “off” digital performance of the
 273 AND gate at steady state was qualitatively and quantitatively assessed by introducing inputs well
 274 above switch points under four different logic conditions (Fig. 2A and 2C). The results show that the
 275 AND gate was only activated in the presence of both inputs with >800au (relative fluorescence unit)
 276 expression increase, as compared to the condition where only single input is present (or no inputs).

277



278

279 Fig. 2. Design and characterization of the biological AND gate.

- 280 A. Design and logic output of Hrp-based AND gate. The AND gate comprises of HrpS and HrpR transcription factors
 281 that are unregulated under the control of pBAD and pRHAB promoters, respectively. In the presence of both inputs
 282 HrpRS jointly bind and induce conformational change in the pHrL promoter, thereby enabling DNA transcription and
 283 the expression of GFP reporter.
 284 B. Steady state profile of the AND gate for various concentrations of arabinose (input A) and rhamnose (input B).
 285 C. Digital performance of AND gate at steady state.
 286 D. Characterization of the Hrp-based AND gate in both high and low copy plasmids. The input devices generating
 287 HrpRS transcription factors and pHrL-GFP reporter module are placed in plasmids of different copy numbers to study
 288 the effect of plasmid copy on precision control and tuning of Hrp-based AND gate.

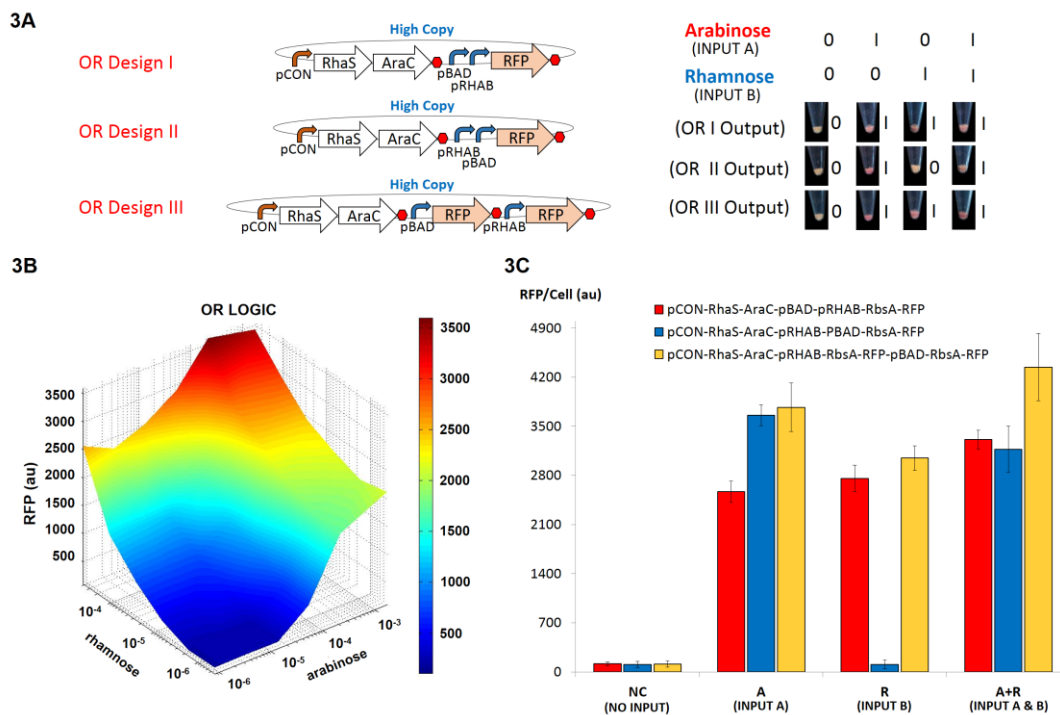
289 Error bars represent the standard deviation of three independent experiments.

290

291 To assess the effect of plasmid copy number on the performance of the AND gate, modules were
 292 constructed which generate the HrpRS transcription activators (pBAD-HrpS-pRHAB-HrpR). This
 293 produces a GFP output (pHrL-GFP) into separate low and high copy plasmids (co-transformed the
 294 plasmids into E. coli cells). The relative GFP output of each system was measured (Fig. 2D). The
 295 results show that the AND gate system with the GFP-producing module in high copy plasmid and
 296 HrpRS transcription activators in low copy plasmid produced a >4 fold greater GFP output than AND

297 gate systems with GFP-producing module in low copy plasmid and HrpRS (as compared to
 298 transcription activators in either low or high copy plasmids). The result indicates that a higher
 299 concentration of HrpRS transcription activators, above the saturation limit of the pHrPL promoter, do
 300 not produce a greater GFP output. It is likely that the transcriptional output of the HrpRS AND gate is
 301 limited by the strength of the weak pHrPL promoter. Hence, the conclusion is that when pHrPL-GFP
 302 module was expressed in high copy plasmids, intracellular availability of pHrPL promoters were
 303 increased - resulting in the amplification of GFP output.

304 Design and Characterisation of OR Logic Gate



305

306 Fig. 3. Design and characterization of biological OR gates.

307 A. The genetic blueprint and logic output of three OR gate designs. Designs I and II are tandem promoters in opposite
 308 arrangement, while design III expresses RFP reporter in two distinct transcripts. Only design I and III are functional
 309 OR gates that generates RFP in the presence of either inputs.

310 B. Steady state profile of OR gate I for various concentrations of arabinose (input A) and rhamnose (input B).

311 C. Digital performance of OR gates at steady state.

312 Error bars represent the standard deviation of three independent experiments.

313

314 Genetic OR gates can be achieved by designing tandem promoter genetic circuits or by expressing
 315 target gene in two discrete expression cassettes. Nonetheless, tandem promoter OR gate circuits
 316 may fail when repression of downstream promoter prevents the proper functioning of the upstream
 317 promoter [38]. To develop the OR logic gate of the half adder, three prototype designs were
 318 constructed; two of which comprised of pBAD and pRHAB promoters in different tandem
 319 arrangements upstream of an RFP reporter gene with strong RBS, and a third design that produces
 320 RFP in two distinct expression cassettes (Fig. 3A). The three OR gate designs were then introduced

321 with input A and B above their switch points and assessed for the respective RFP outputs (Fig. 3A
322 and 3C). The results show that designs I and III are functional OR gates with >2500au higher RFP
323 expression when either or both inputs are present. In our computational model, the total amount of
324 RFP expression was approximated by the sum of RFP amounts produced from individual pBAD and
325 pRHAB promoters. Although the model predicts well from low to medium range induction levels, our
326 assumption was not valid at very high induction levels, in which lesser RFP expression was observed
327 than predicted. It is possible that at very high induction level, the transcription and translation
328 machinery in cells are fully saturated, thereby imposing metabolic burden on the cells and limiting
329 protein production [39]. The OR gate design II, which composed of pRHAB promoter upstream of
330 pBAD promoter and RFP reporter was activated only in the presence of rhamnose, but not arabinose.
331 Our results agree with previous finding that no expression was detected when pBAD promoter was
332 fused downstream of tetracycline-inducible pTET promoter and upstream of a YFP reporter [38]. The
333 conclusion is that it is likely that this observation is an effect of the AraC transcription factor - which
334 can function as both repressor and activator. In the absence of arabinose, AraC when over expressed,
335 remains bound to operator sites that induce DNA looping of the pBAD promoter, thereby obstructing
336 the elongation of mRNA by initiated RNA polymerase. As will be shown in the next section, in order to
337 layer OR gate design I into other logic devices, the construct was characterised for its steady state
338 profile by titrating with varying concentration of arabinose and rhamnose (Fig. 3B). Results of the
339 engineered OR gate generally correlated well with our steady state computational model
340 (Supplementary Fig. 12), which was applied to match biological modules making up the OR gate.

341 **Genetic Context Effect of σ 54-dependent pHrpL promoter**

342 To enable sufficient expression of the λ CI repressor by an AND gate system, the gene encoding for
343 λ CI repressor was assembled downstream of σ 54-dependent pHrpL promoter on a high copy plasmid.
344 Fortuitously, we discovered that pHrpL promoter located downstream of another pHrpL expression
345 cassette can be turned on even in the absence of its cognate HrpRS transcription factors
346 (Supplementary Fig. 5C). The converse is not true for an upstream pHrpL promoter (Supplementary
347 Fig. 5B). Negative controls with just the GFP reporter or RBS- λ CI gene upstream of pHrpL-GFP
348 module confirmed that pHrpL promoter alone is not leaky and that cryptic promoter is absent in the
349 λ CI gene (Supplementary Fig. 5A and 5D). To buffer against this genetic context dependent effect of
350 the pHrpL promoters, pHrpL-GFP and pHrpL- λ CI modules were assembled on separate plasmids.
351 This successfully prevented the genetic interference of both pHrpL expression modules on each other
352 (Supplementary Fig. 5E and 5F). Supplementary Fig. 5G shows a quantitative assessment of pHrpL
353 promoter activation due to the presence of another upstream pHrpL promoter and the use of plasmids
354 as genetic insulators.

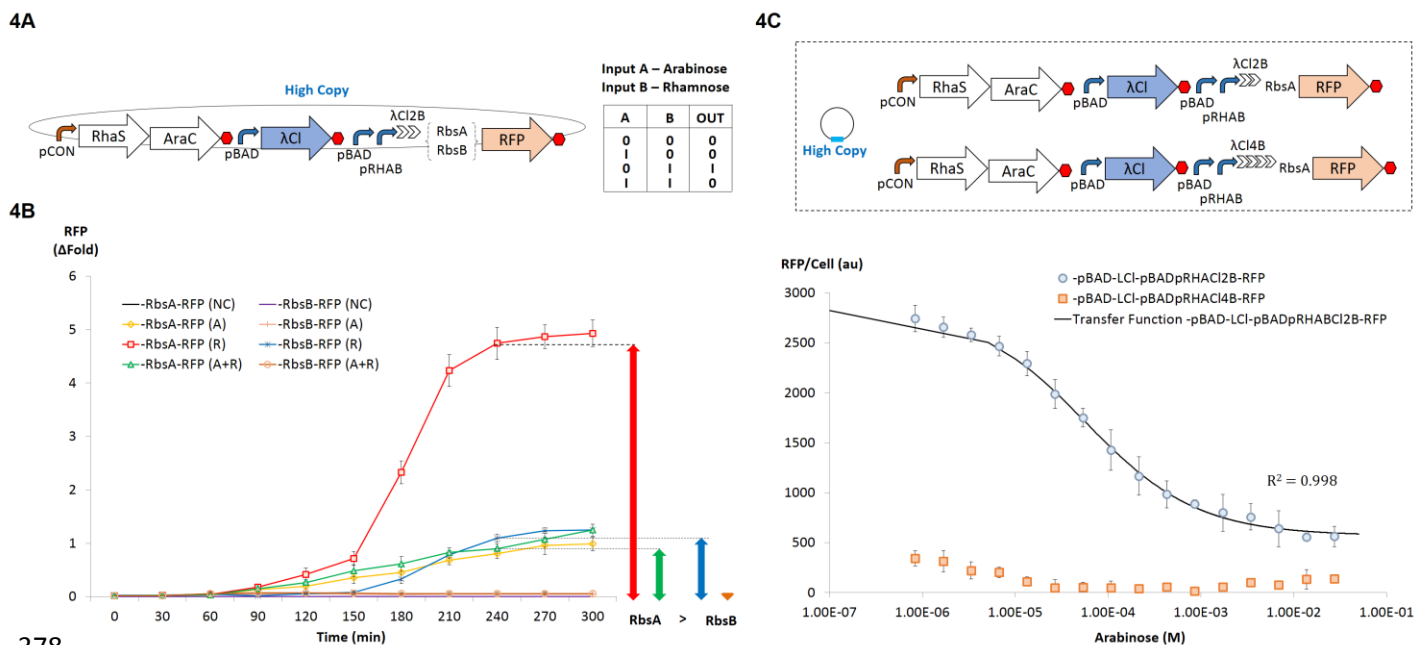
355 **Design and Characterisation of NOT and NIMPLY Logic Gates**

356 As part of the development of XOR logic operations of the half adder, repressor binding sites are
357 required downstream of the OR gate promoters. To examine the minimal number of λ CI repressor
358 binding sites required for effective repression, single λ CI operator site and dual λ CI operator sites of

359 perfect dyad symmetry were fused downstream of pBAD promoter, before the RFP gene [40]. The
 360 repressibility of both circuits was tested by generating λ CI repressors from HrpRS AND gate in a
 361 separate plasmid. Negligible repression was observed when only one λ CI repressor operator site was
 362 present. In the presence of two operator sites of perfect dyad symmetry, RFP expression from pBAD
 363 promoter was greatly attenuated - even when λ CI repressor was not synthesized. We postulate that
 364 the observed reduction of RFP expression might be caused by the presence of secondary hairpin
 365 structures immediately downstream of TSS acting as *pseudo* transcription terminator or locking RBS
 366 in conformations that prevented translation initiation (Supplementary Fig. 6A).

367 In order to examine this further, random mutagenesis on the natural sequence of the λ CI repressor
 368 operator sites were performed and screened for mutants with significant difference in RFP expression
 369 levels, in the absence and presence of λ CI repressor. Accordingly, an evolved candidate (CI2B) with 4
 370 mutations in the inverted sequence of the λ CI repressor binding (Supplementary Fig. 6B) was
 371 obtained. Sequence comparison with the original λ CI repressor binding sites (CI2A) with the evolved
 372 candidate revealed that the directed evolution process had eliminated the effect of secondary hairpin
 373 structures from 7 to 3. Next, the efficiency of λ CI-mediated transcription termination in the context of a
 374 genetic NIMPLY gate was studied. This was achieved by placing repressor binding sites directly
 375 downstream of tandem pBAD-pRHAB promoters and generating λ CI repressors from a separate
 376 pBAD expression cassette.

377



378

379 Fig. 4. Design and characterization of the biological NIMPLY gate.

380 A. Genetic blueprint and logic output of NIMPLY gate. The NIMPLY gate is designed by incorporating synthetic lambda
 381 repressor binding sites downstream of OR gate promoters and regulating the expression of lambda repressors
 382 through the pBAD promoter. RFP is expressed only in the presence of input B, rhamnose.

383 B. Characterization of NIMPLY gate with different ribosome binding sites. At steady state NIMPLY gate which utilizes a
 384 weaker ribosome binding site (RbsB) directly upstream of the RFP reporter (denoted by black stars, orange circles

385 and purple crosses) exhibits better control and reduced expression leak, as compared to the NIMPLY gate design
386 that contains a stronger ribosome binding site (denoted by red squares, green triangles and blue diamonds).
387 Expression leakiness in circuits with strong and weak ribosome binding sites after 4 hours are denoted by green and
388 orange arrowheads, respectively. Constructs that were singly induced with input B, induced with both inputs A and
389 B, and uninduced are represented by R, A+R and NC as shown.

390 C. Characterization of NIMPLY gates with two (blue circles) and four (red squares) lambda repressor binding sites. The
391 black line represents empirically-derived transfer function for the construct with dual lambda repressor binding sites,
392 as described by the equation provided. Constructs were induced with a fixed amount of rhamnose (input B) and
393 titrated with various concentrations of arabinose (input A). An increased number of repressor binding sites disrupted
394 the NIMPLY gate, possibly due to pronounced effect of 5' mRNA secondary structures.

395 Error bars represent standard deviation of three independent experiments.

396

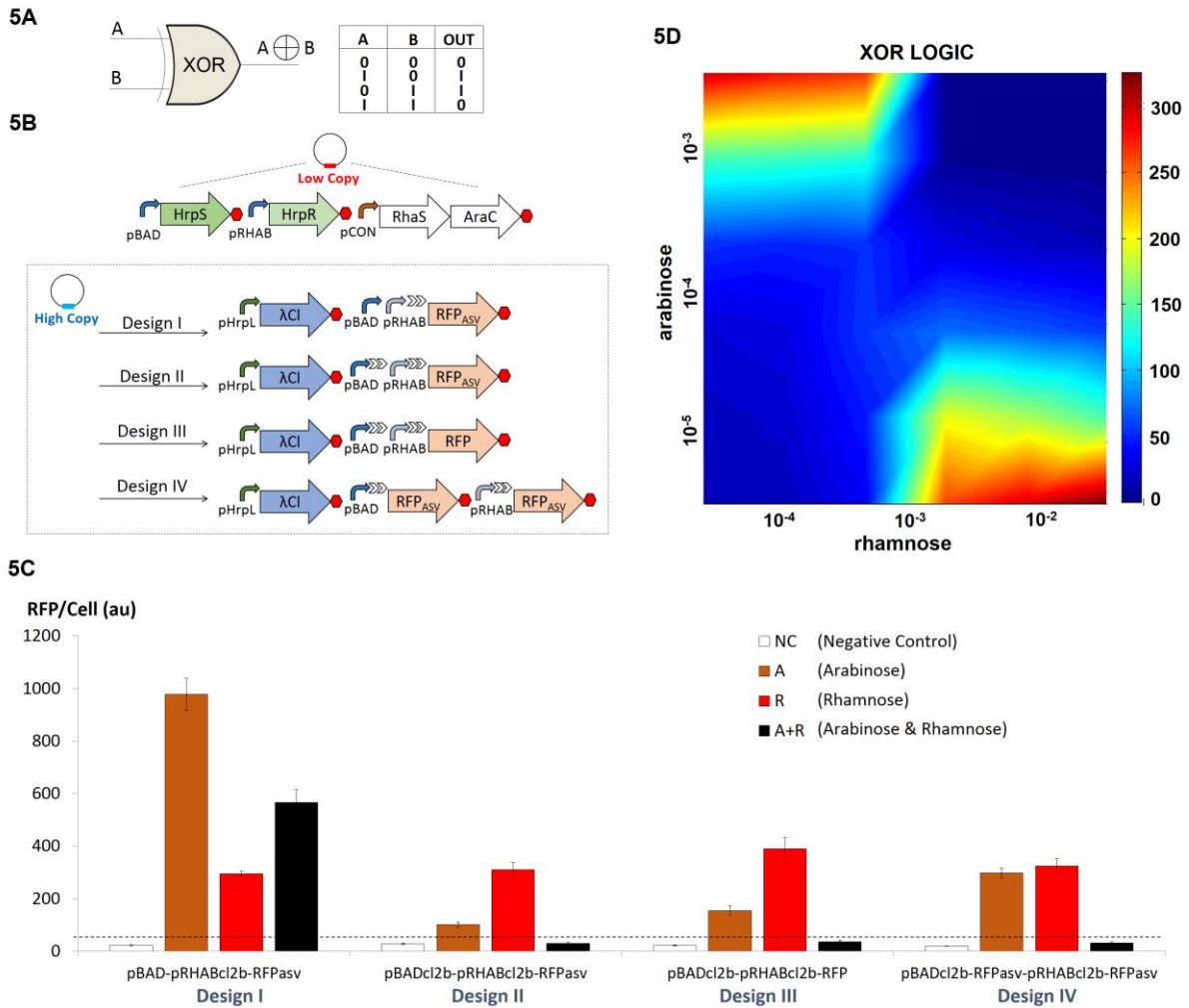
397 Two NIMPLY logic circuits were developed which generated RFP transcripts with strong and weak
398 RBS. Both NIMPLY logic circuits were then tested in the presence and absence of input A (arabinose)
399 over time with input B (rhamnose), both above switch point (Fig. 4A). Temporal analysis of the
400 NIMPLY logic circuits showed that there was no significant delay in layering NOT gate downstream of
401 an OR gate (Fig. 4B). However, apparent delay in total amount of mature RFP was observed when a
402 weaker RBS was used to initiate the translation of RFP gene. The results also showed that while
403 NIMPLY logic can be achieved from both circuits, the system with the strong RBS exhibited a higher
404 order of expression and leakiness as compared to that which translated RFP from weaker RBS. This
405 leads to the conclusion that the choice of a particular RBS can be used as a signal moderation
406 technique in order to achieve a balance between precision tuning and output gain in layered logic
407 gates. In an attempt to alleviate expression leakiness from the NIMPLY gate with strong RBS, an
408 additional pair of λ CI repressor binding sites with imperfect dyad symmetry were introduced
409 downstream of pBAD-pRHAB-CI2B, and before the RBS-RFP module. However, the presence of 4
410 λ CI binding sites completely inhibited RFP expression, resulting in the failure of the NIMPLY gate (Fig.
411 4C). It is likely that this failure could be an effect of pronounced 5' UTR secondary structures formed
412 due to the repeated use of identical λ CI repressor binding sites.

413 **Design and Characterisation of XOR Logic Gate**

414 In order to develop the XOR component of the half adder, we assimilated and tested a combination of
415 AND, OR, and NOT logic gates in four different genetic circuits. In all the designs HrpRS transcription
416 activators were expressed from low copy plasmid to drive the synthesis of λ CI repressors from pHrpL
417 promoter in high copy plasmids (Fig. 5B). OR and NOT biological modules were assembled in the
418 same high copy plasmid downstream of pHrpL- λ CI module. In design I, an OR gate comprising a
419 tandem arrangement of pBAD, pRHAB and λ CI repressor binding sites was used to express *ssrA*-
420 tagged, short-lived RFP (RFP_{asv}) - one of the most well characterised protein degradation system in *E.*
421 *coli* [41]. In design II we created hybrid promoters of pBAD and pRHAB by incorporating λ CI binding
422 sites downstream of both promoters before connecting them in tandem to elicit hypothetical OR logic
423 as similar to design I. Design III was modified from design II to express long-lived RFP. To overcome
424 possible complications from 5'UTR secondary structures - due to presence of multiple λ CI binding

425 sites within the same mRNA transcript, design IV, which comprised of synthetic hybrid promoters of
 426 pBAD-CI2B and pRHAB-CI2B expressing RFP_{asv} in two discrete expression cassettes was also
 427 developed.

428



429

430 Fig. 5. Design and characterization of biological XOR gates.

- 431 A. The logic output of XOR gate.
- 432 B. Genetic blueprint of four biological XOR gate designs. The XOR gate comprises of serially layered AND, NOT and
 433 OR gates. HrpRS transcription factors are carried in a low copy plasmid, while pHrpL-λCI and distinct modules of OR
 434 gates with lambda repressor binding sites expressing RFP reporter are carried in high copy plasmids. Design I
 435 comprises tandem promoters with repressor binding sites downstream of pRHAB promoter and a RFP reporter
 436 engineered with the ASV protein degradation tag. Designs II and III comprise tandem promoters with repressor
 437 binding sites downstream of each promoter and RFP with and without the ASV degradation tag respectively. Design
 438 IV is modified from design II with RFP expressed in two disparate transcripts.
- 439 C. Digital performance of various designs of biological XOR gates at steady state.
- 440 D. The steady state profile of XOR gate IV for various concentrations of arabinose (input A) and rhamnose (input B).
 441 Error bars represent the standard deviation of four independent experiments.

442

443 Accordingly, only design IV was able to achieve well-balanced outputs which accurately described
444 XOR logic operations (Fig. 5C). While design I demonstrated the strong suppression of RFP output in
445 the presence of both inputs (arabinose and rhamnose), when characterised as an NIMPLY gate (as
446 described earlier), the same design failed to function in the context of XOR gate in which a weaker
447 pHrpL promoter was used to drive the synthesis λ CI repressors instead of the strong pBAD promoter.
448 Interestingly, the results imply that when employing transcription repressors as molecular blockers to
449 mRNA elongation, a higher concentration of λ CI molecules is needed to completely suppress
450 transcription as λ CI binding sites are engineered further away from the transcription start site. This
451 observation may be an effect of RNAP gaining momentum as it runs down template DNA to perform
452 transcription, inadvertently enabling RNAP to continue its course of action as a result of the
453 inadequacy of “molecular brakes”.

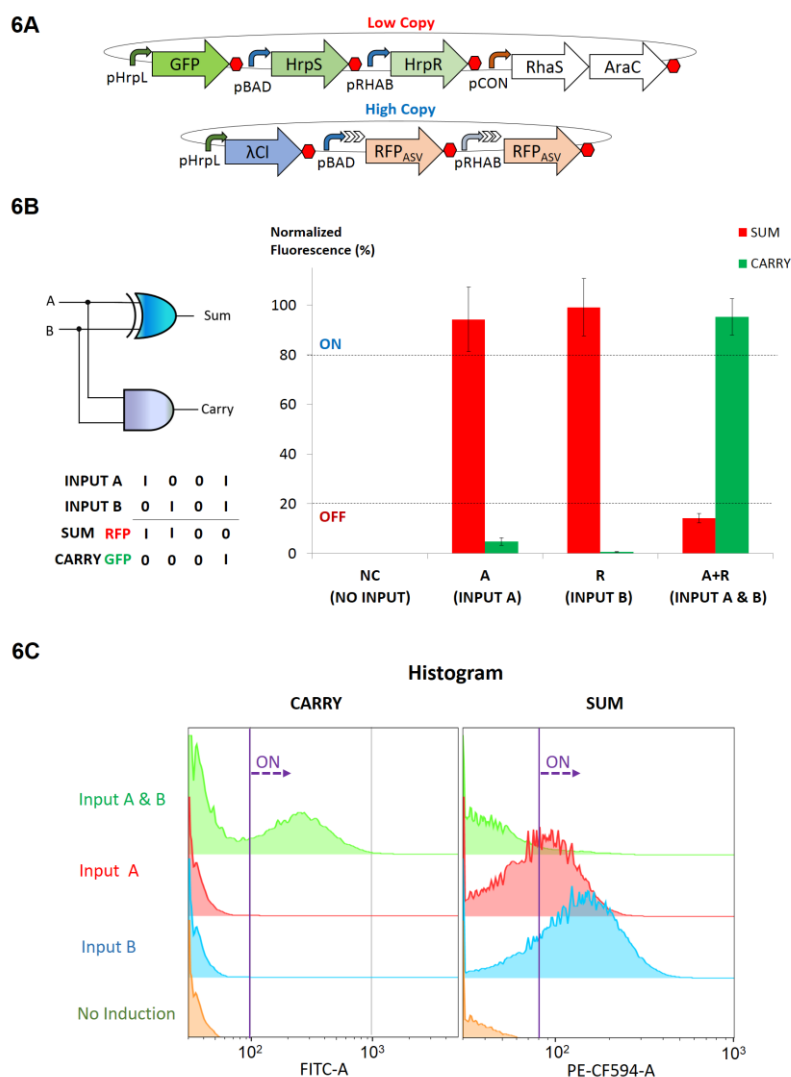
454 While designs II and III, that were developed with λ CI binding sites downstream of both pBAD and
455 pRHAB promoters, exhibited a slight semblance of XOR logic operations, the presence of multiple,
456 repeated sequences of λ CI binding sites in the transcript generated from the pBAD promoter greatly
457 reduced the RFP output from Input A. Using untagged RFP gene in design III led to slight increase in
458 overall RFP output but did not alleviate the signal balancing issue. The result implies that 5'UTR
459 structural effect is more dominant than RFP half-life in determining the success of layered XOR gate.
460 In order to apply the XOR gate in the implementation of the half adder, design IV was characterised
461 for its steady state profile by titrating with varying concentration of arabinose and rhamnose as shown
462 in Fig. 5D. It is noteworthy that the XOR gate developed in this work possesses higher single cell
463 computational capability as compared to that achieved by *Tamsir* and colleagues using a network of
464 inter-communicating cells [38], hence circumventing problems associated with cell-cell communication.

465 **Design and Characterisation of Single Cell Half Adder and Half Subtractor**

466 The half adder computes dual inputs with both AND and XOR logic operations to generate CARRY
467 and SUM output, respectively. Building on bio-logical devices that were modularised and rigorously
468 characterised earlier, we co-transformed constructs which produce GFP (CARRY) from HrpRS AND
469 gate in low copy plasmid, RFP_{asv} (SUM) from hybrid promoters pBAD-CI2B and pRHAB-CI2B and λ CI
470 repressors from pHrpL promoter in high copy plasmid into *E. coli* (Fig. 6A). To study the digital
471 performance of the single cell half adder, we characterised the system at both the population and
472 single cell levels by microplate fluorescent assay (Fig. 6B) and flow cytometry (Fig. 6C,
473 Supplementary Fig. 7) for four different logic conditions. The results show that the engineered cells
474 exhibited robust and digital-like performance with minor expression leak (< 20%) in XOR output when
475 both inputs were present. While previous characterisation with standalone XOR gates displayed near
476 perfect XOR outputs, parallel implementation of both AND and XOR logic gates in half adder led to
477 probable competition for HrpRS transcription activators by pHrpL promoters in both low and high copy
478 plasmids - which is suggestive of expression shunting in competitive transcription dynamics [42]. In
479 other words, the availability of HrpRS activators are divided between the pHrpL-GFP module in low
480 copy plasmid and pHrpL- λ CI module in high copy plasmid, thus causing both AND and XOR gates to
481 perform below par compared to when they are operating individually. To affirm the hypothesis, we

482 examined the AND output of standalone AND gate with the AND output of the half adder using
 483 microplate fluorescent assay. The results showed that the GFP output of isolated AND gate was
 484 approximately 7 times stronger than that of half adder's AND gate, thus confirming our hypothesis
 485 (Supplementary Fig. 8). It is noteworthy, that the reduced expression of GFP did not affect the overall
 486 performance of the half adder as effective half adder logic operations were still achieved. In the
 487 current single cell half adder, the engineered cells exhibited relatively healthy growth with the same
 488 order of viable cells ($\sim 10^9$ cfu/ml) in both induced and uninduced cell cultures (Supplementary Fig. 9).
 489 Nevertheless, as genetic complexity and heterologous expression increased, a concomitant increase
 490 in the metabolic burden in the *E. coli* cell was also observed.

491



492

493 Fig. 6. Design and characterization of the biological half adder.

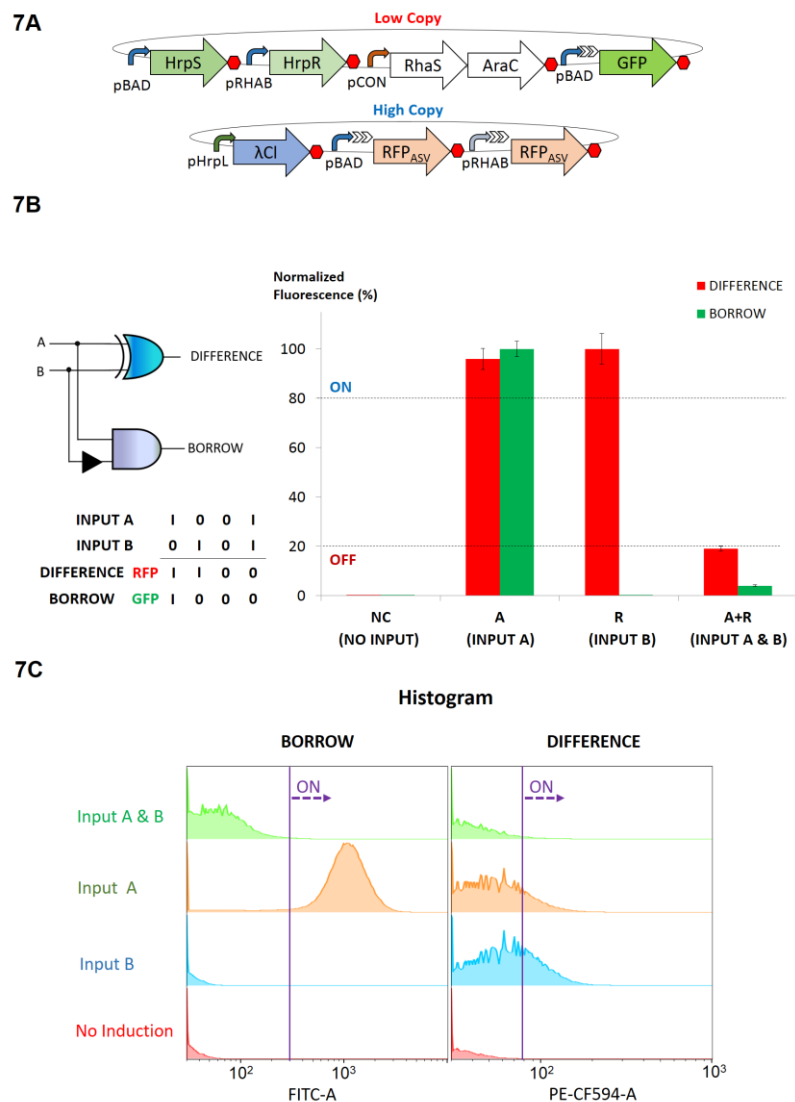
- 494 A. Genetic blueprint of the half adder.
 495 B. Digital performance of the half adder at steady state.
 496 C. Flow cytometry analysis of the half adder. The Y axis coordinate represents population count, while FITC-A and PE-
 497 CF594-A represent channels that detects GFP and RFP fluorescence respectively. Population shifts to the right
 498 represent ON behaviour.

499 Error bars represent the standard deviation of four independent experiments.

500

501 To demonstrate the modularity of our approach, we also developed single cell half subtractor by
 502 performing slight modifications to the genetic circuits that formed the basis of the half adder.
 503 Specifically, GFP, which exemplifies BORROW output, was produced from the hybrid promoter
 504 pBAD-CI2B in the low copy plasmid instead of the pHrpL promoter (Fig. 7A). As above, the construct
 505 which generated the BORROW output (GFP) and that which generated the DIFFERENCE output
 506 (RFP) were co-transformed into *E. coli* cells. Characterisation was undertaken at both the population
 507 and single cell levels by microplate fluorescent assay (Fig. 7B) and flow cytometry (Fig. 7C) under
 508 four different logic conditions. The results showed that the engineered cells functioned as effective
 509 biological half subtractors, producing GFP only in the presence of input A and RFP in the presence of
 510 input A or B, but not when both inputs were present.

511



512

513 Fig. 7. Design and characterization of the biological half subtractor.
514 A. Genetic blueprint of the half subtractor.
515 B. Digital performance of half subtractor at steady state.
516 C. Flow cytometry analysis of the half adder. Y axis coordinate represents population count, while FITC-A and PE-
517 CF594-A represent channels that detects GFP and RFP fluorescence, respectively. Population shifts to the right
518 represent ON behaviour.
519 Error bars represent the standard deviation of four independent experiments.

520

521 **DISCUSSION**

522 Logic gates are the basis of all electronic digital devices from mobile phones, to microprocessors, to
523 computers. They are therefore the basis of the processing of information and control systems.
524 Similarly, the development of biologically based logic gates and logical devices has major potential in
525 terms of information processing and control. The design and testing of a half adder, which is the
526 subject of this paper, is seen as a significant step in the development of biological logical devices,
527 comprising multiple gates that work stably and in unison. Immediate areas of application are in
528 advanced biosensors. In the longer term, there is the potential to development of biologically-based
529 devices for information processing and control, for example in the application of human-imposed intra-
530 cellular control. In the underlying strategy of the paper is one of applying systematic design through
531 the application of engineering principles [43]. Using a forward engineering approach that is supported
532 by modelling and rigorous characterisation, independent modules that enable programmable digital
533 operations in prokaryotic cells, including simple genetic switches, AND, OR and NOT logic operations
534 were systematically assembled and characterised. AND, OR and NOT logic gates were then layered
535 in both parallel and serial arrangements to generate a repertoire of cellular Boolean operations that
536 include NIMPLY, XOR, half adder and half subtractor logic operations. Using a bottom up approach
537 for constructing biological systems of increasing complexity we assessed genetic architectures that
538 led to genetic context dependent effects. On this basis, the significance of each design on the overall
539 digital performance of programmable logic gates in engineered cells was studied, leading to the
540 compilation of a comprehensive set of guidelines for troubleshooting synthetic genetic circuits (Table
541 1). This work together with recent studies conducted elsewhere, highlight the importance of
542 modularity and characterisation during the systematic layering of multiple biological devices [10, 44,
543 45].

544 Overall, the presence of secondary structures in 5'-UTR of mRNA affects genetic expression most.
545 We discovered that the presence of seven consecutive hairpins immediately downstream of promoter
546 transcription start site would cause severe impediment of gene expression. Although OR gate design
547 made up of tandem promoters can be subjected to the undesirable effects of 5'-UTR secondary
548 structure, we showed that the effect is not pronounced in the digital performance of the OR logic when
549 the promoters and DNA operator sites involved are of markedly different DNA sequences. The OR
550 gate design that comprises a separate gene expression cassette also reliably demonstrates digital
551 operation. However, the involvement of larger DNA modules and repetitive use of transcription
552 terminators that are rich in secondary hairpin structures may impede system assembly in terms of

553 construction efficiency and accuracy. Where identical DNA sequences are incorporated in a single
554 mRNA transcript, as shown in a design II and III of XOR gate, the effect of 5'-UTR secondary
555 structure preventing gene expression is significantly more pronounced. Thus, it is proposed that XOR
556 gate logic in layered genetic circuits should be designed with two discrete expression cassettes
557 instead of employing a tandem promoter circuit design. It would also be interesting to test if RNA
558 processing tools can be employed in multiplex mode to insulate the myriad of biological devices from
559 RNA genetic context dependent effects in layered genetic circuits concurrently.

560 Perhaps of particular interest, we discovered that $\sigma 54$ promoters can exhibit genetic context
561 dependent effects if two $\sigma 54$ promoters are placed close to each other. Previously, $\sigma 54$ -dependent
562 NtrC-binding promoters have been reported. These promoters permit transcription *in vitro* in the
563 absence of enhancer-binding proteins and ATP under conditions that promote DNA melting. These
564 include DNA supercoiling, temperature rise and lower ionic strength, or when characteristic point
565 mutations are implemented on the $\sigma 54$ protein [46, 47]. In this paper, we show that an upstream $\sigma 54$
566 pHrpL promoter could also activate downstream pHrpL promoter *in vivo* if the two promoters are in
567 close proximity - possibly as a result of plasmid DNA supercoiling. This undesired switched-on activity
568 can be avoided by designing pHrpL expression modules in different plasmids, ie to use plasmid as
569 genetic buffers to insulate such genetic context dependent effects.

570 While recombinases have been intelligently crafted into Boolean logic gates with DNA-encoded
571 memory functions, it is important to note that biosensors connected in AND, OR and XOR operations
572 with recombinase-based logic gates may not be able to distinguish inputs from different environments
573 and provide the desired response. For example, a probiotic that is genetically programmed in AND
574 logic to sense two inputs such as hypoxia and low pH may be activated for hypoxia and low pH
575 signals in two different locations, as compared to sensing both signals *in situ*. The same may be
576 applicable for other logic operations with recombinase-based logic gates. Thus, layered genetic
577 circuits that are capable of sensing and providing location-sensitive Boolean logic operations are still
578 useful in programming cellular behaviour. Of particular interest is a combination of layered genetic
579 circuits, with the synthesis of recombinases as intermediary output, this may provide a novel and
580 better platform for programmable cellular behaviour in terms of both accuracy and memory.

581 With the exceptions of a notable few [19, 48, 49], most studies of synthetic biological systems are
582 centred on the development of rational engineering approaches, reporting successful and
583 advantageous aspects of the engineered systems, with lesser focus on reporting failure modes and
584 compiling the engineering solutions applied to troubleshoot system failures. As synthetic biology
585 moves forward with greater focus on scaling the complexity of engineered genetic circuits, studies
586 which thoroughly evaluate failure modes and engineering solutions will serve as important references
587 for future design and development of synthetic biological systems.

588

589 **ACKNOWLEDGEMENT**

590 We are grateful to P. Freemont, K. Jensen, C. Hirst and F. Jonas from Imperial College London for
591 suggestions, M.W. Chang from the University of Singapore for experimental support and the use of
592 flow cytometer for the work, and B.J. Wang for the kind donation of plasmids containing *hrpS*, *hrpR*
593 and *pHrpL* promoter. We would also like to thank the anonymous reviewers for their comments on this
594 paper.

595 **FUNDING**

596 A.W is funded by NTU-IC joint PhD scholarship programme. R.I.K would like to acknowledge the
597 financial support of the UK Engineering and Physical Sciences Research Council for the project, and
598 C.L.P would like to acknowledge the financial support of the Ministry of Education of Singapore (AcRF
599 ARC43/13) for the project.

600 **REFERENCES**

- 601 1. Mayo AE, Setty Y, Shavit S, Zaslaver A, Alon U: **Plasticity of the cis-regulatory input function**
602 **of a gene.** *PLoS Biol* 2006, **4**(4):e45.
- 603 2. Peter IS, Faure E, Davidson EH: **Predictive computation of genomic logic processing**
604 **functions in embryonic development.** *Proceedings of the National Academy of Sciences of*
605 *the United States of America* 2012, **109**(41):16434-16442.
- 606 3. Thomas R: **Boolean formalization of genetic control circuits.** *Journal of theoretical biology*
607 1973, **42**(3):563-585.
- 608 4. Khalil AS, Lu TK, Bashor CJ, Ramirez CL, Pyenson NC, Joung JK, Collins JJ: **A synthetic biology**
609 **framework for programming eukaryotic transcription functions.** *Cell* 2012, **150**(3):647-658.
- 610 5. Lou C, Stanton B, Chen Y-J, Munsky B, Voigt CA: **Ribozyme-based insulator parts buffer**
611 **synthetic circuits from genetic context.** *Nat Biotechnol* 2012, **30**(11):1137-1142.
- 612 6. Mutalik VK, Guimaraes JC, Cambray G, Lam C, Christoffersen MJ, Mai Q-A, Tran AB, Paull M,
613 Keasling JD, Arkin AP *et al*: **Precise and reliable gene expression via standard transcription**
614 **and translation initiation elements.** *Nature Methods* 2013, **10**(4):354-360.
- 615 7. Cardinale S, Joachimiak Marcin P, Arkin Adam P: **Effects of Genetic Variation on the E. coli**
616 **Host-Circuit Interface.** *Cell Reports* 2013, **4**(2):231-237.
- 617 8. Cardinale S, Arkin AP: **Contextualizing context for synthetic biology – identifying causes of**
618 **failure of synthetic biological systems.** *Biotechnology Journal* 2012, **7**(7):856-866.
- 619 9. Rackham O, Chin JW: **A network of orthogonal ribosome-mRNA pairs.** *Nat Chem Biol* 2005,
620 **1**(3):159-166.
- 621 10. Moon TS, Lou C, Tamsir A, Stanton BC, Voigt CA: **Genetic programs constructed from**
622 **layered logic gates in single cells.** *Nature* 2012, **491**(7423):249-253.
- 623 11. Lucks JB, Qi L, Mutalik VK, Wang D, Arkin AP: **Versatile RNA-sensing transcriptional**
624 **regulators for engineering genetic networks.** *Proceedings of the National Academy of*
625 *Sciences of the United States of America* 2011, **108**(21):8617-8622.
- 626 12. Wang B, Kitney RI, Joly N, Buck M: **Engineering modular and orthogonal genetic logic gates**
627 **for robust digital-like synthetic biology.** *Nature Communications* 2011, **2**.
- 628 13. An W, Chin JW: **Synthesis of orthogonal transcription-translation networks.** *Proceedings of*
629 *the National Academy of Sciences of the United States of America* 2009, **106**(21):8477-8482.
- 630 14. Auslander S, Auslander D, Muller M, Wieland M, Fussenegger M: **Programmable single-cell**
631 **mammalian biocomputers.** *Nature* 2012, **487**:123-127.

- 632 15. Siuti P, Yazbek J, Lu TK: **Synthetic circuits integrating logic and memory in living cells.** *Nat*
633 *Biotechnol* 2013, **31**(5):448-452.
- 634 16. Bonnet J, Yin P, Ortiz ME, Subsoontorn P, Endy D: **Amplifying Genetic Logic Gates.** *Science*
635 2013, **340**(6132):599-603.
- 636 17. Gardner TS, Cantor CR, Collins JJ: **Construction of a genetic toggle switch in Escherichia coli.**
637 *Nature* 2000, **403**(6767):339-342.
- 638 18. Friedland A, Lu T, Wang X, Shi D, Church G, Collins J: **Synthetic gene networks that count.**
639 *Science* 2009, **324**:1199 - 1202.
- 640 19. Bonnet J, Subsoontorn P, Endy D: **Rewritable digital data storage in live cells via engineered**
641 **control of recombination directionality.** *Proceedings of the National Academy of Sciences of*
642 *the United States of America* 2012, **109**(23):8884-8889.
- 643 20. Qi L, Haurwitz RE, Shao W, Doudna JA, Arkin AP: **RNA processing enables predictable**
644 **programming of gene expression.** *Nat Biotechnol* 2012, **30**(10):1002-1006.
- 645 21. Nikel PI, Martinez-Garcia E, de Lorenzo V: **Biotechnological domestication of**
646 **pseudomonads using synthetic biology.** *Nature Reviews Microbiology* 2014, **12**(5):368-379.
- 647 22. Chen ZY, Guo LL, Zhang YQ, Walzem RL, Pendergast JS, Printz RL, Morris LC, Matafonova E,
648 Stien X, Kang L *et al*: **Incorporation of therapeutically modified bacteria into gut microbiota**
649 **inhibits obesity.** *J Clin Invest* 2014, **124**(8):3391-3406.
- 650 23. Xiang S, Fruehauf J, Li CJ: **Short hairpin RNA-expressing bacteria elicit RNA interference in**
651 **mammals.** *Nat Biotechnol* 2006, **24**(6):697-702.
- 652 24. Duan F, March JC: **Engineered bacterial communication prevents Vibrio cholerae virulence**
653 **in an infant mouse model.** *Proceedings of the National Academy of Sciences of the United*
654 *States of America* 2010, **107**(25):11260-11264.
- 655 25. Saeidi N, Wong CK, Lo TM, Nguyen HX, Ling H, Leong SSJ, Poh CL, Chang MW: **Engineering**
656 **microbes to sense and eradicate Pseudomonas aeruginosa, a human pathogen.** *Mol Syst*
657 *Biol* 2011, **7**(1):521.
- 658 26. Callura J, Dwyer D, Isaacs F, Cantor C, Collins J: **Tracking, tuning, and terminating microbial**
659 **physiology using synthetic riboregulators.** *Proceedings of the National Academy of Sciences*
660 *of the United States of America* 2010, **107**:15898 - 15903.
- 661 27. Callura JM, Cantor CR, Collins JJ: **Genetic switchboard for synthetic biology applications.**
662 *Proceedings of the National Academy of Sciences of the United States of America* 2012,
663 **109**(15):5850-5855.
- 664 28. Temme K, Hill R, Segall-Shapiro TH, Moser F, Voigt CA: **Modular control of multiple**
665 **pathways using engineered orthogonal T7 polymerases.** *Nucleic Acids Res* 2012,
666 **40**(17):8773-8781.
- 667 29. Collins CH, Leadbetter JR, Arnold FH: **Dual selection enhances the signaling specificity of a**
668 **variant of the quorum-sensing transcriptional activator LuxR.** *Nat Biotechnol* 2006,
669 **24**(6):708-712.
- 670 30. Canton B, Labno A, Endy D: **Refinement and standardization of synthetic biological parts**
671 **and devices.** *Nature Biotechnology* 2008, **26**:787 - 793.
- 672 31. Lee SK, Chou HH, Pflieger BF, Newman JD, Yoshikuni Y, Keasling JD: **Directed evolution of**
673 **AraC for improved compatibility of arabinose- and lactose-inducible promoters.** *Appl*
674 *Environ Microb* 2007, **73**(18):5711-5715.
- 675 32. Laub MT, Goulian M: **Specificity in two-component signal transduction pathways.** *Annu Rev*
676 *Genet* 2007, **41**:121-145.
- 677 33. Yu BJ, Kang KH, Lee JH, Sung BH, Kim MS, Kim SC: **Rapid and efficient construction of**
678 **markerless deletions in the Escherichia coli genome.** *Nucleic Acids Res* 2008, **36**(14):e84.
- 679 34. Bloodworth RAM, Gislason AS, Cardona ST: **Burkholderia cenocepacia conditional growth**
680 **mutant library created by random promoter replacement of essential genes.**
681 *MicrobiologyOpen* 2013, **2**(2):243-258.

- 682 35. Cardona ST, Mueller CL, Valvano MA: **Identification of Essential Operons with a Rhamnose-**
683 **Inducible Promoter in Burkholderia cenocepacia.** *Appl Environ Microb* 2006, **72**(4):2547-
684 2555.
- 685 36. Shis DL, Bennett MR: **Library of synthetic transcriptional AND gates built with split T7 RNA**
686 **polymerase mutants.** *Proceedings of the National Academy of Sciences of the United States*
687 *of America* 2013, **110**(13):5028-5033.
- 688 37. Anderson JC, Voigt CA, Arkin AP: **Environmental signal integration by a modular AND gate.**
689 *Mol Syst Biol* 2007, **3**:133.
- 690 38. Tamsir A, Tabor JJ, Voigt CA: **Robust multicellular computing using genetically encoded**
691 **NOR gates and chemical 'wires'.** *Nature* 2011, **469**(7329):212-215.
- 692 39. Glick BR: **Metabolic load and heterologous gene expression.** *Biotechnology Advances* 1995,
693 **13**(2):247-261.
- 694 40. Benson N, Sugiono P, Youderian P: **DNA sequence determinants of lambda repressor**
695 **binding in vivo.** *Genetics* 1988, **118**(1):21-29.
- 696 41. Andersen JB, Sternberg C, Poulsen LK, Bjørn SP, Givskov M, Molin S: **New Unstable Variants**
697 **of Green Fluorescent Protein for Studies of Transient Gene Expression in Bacteria.** *Appl*
698 *Environ Microb* 1998, **64**(6):2240-2246.
- 699 42. Daniel R, Rubens JR, Sarpeshkar R, Lu TK: **Synthetic analog computation in living cells.**
700 *Nature* 2013, **497**(7451):619-623.
- 701 43. Kitney R, Freemont P: **Synthetic biology - the state of play.** *Febs Lett* 2012, **586**(15):2029-
702 2036.
- 703 44. Tabor J, Salis H, Simpson Z, Chevalier A, Levskaya A, Marcotte E, Voigt C, Ellington A: **A**
704 **synthetic genetic edge detection program.** *Cell* 2009, **137**:1272 - 1281.
- 705 45. Zhang H, Lin M, Shi H, Ji W, Huang L, Zhang X, Shen S, Gao R, Wu S, Tian C *et al*:
706 **Programming a Pavlovian-like conditioning circuit in Escherichia coli.** *Nature*
707 *Communications* 2014, **5**.
- 708 46. Wang JT, Syed A, Gralla JD: **Multiple pathways to bypass the enhancer requirement of**
709 **sigma 54 RNA polymerase: Roles for DNA and protein determinants.** *Proceedings of the*
710 *National Academy of Sciences of the United States of America* 1997, **94**(18):9538-9543.
- 711 47. Wang JT, Syed A, Hsieh M, Gralla JD: **Converting Escherichia coli RNA polymerase into an**
712 **enhancer-responsive enzyme: role of an NH2-terminal leucine patch in sigma 54.** *Science*
713 1995, **270**(5238):992-994.
- 714 48. Brophy JAN, Voigt CA: **Principles of genetic circuit design.** *Nat Methods* 2014, **11**(5):508-520.
- 715 49. Slusarczyk AL, Lin A, Weiss R: **Foundations for the design and implementation of synthetic**
716 **genetic circuits.** *Nature Reviews Genetics* 2012, **13**(6):406-420.
- 717 50. Rhodius VA, Segall-Shapiro TH, Sharon BD, Ghodasara A, Orlova E, Tabakh H, Burkhardt DH,
718 Clancy K, Peterson TC, Gross CA *et al*: **Design of orthogonal genetic switches based on a**
719 **crosstalk map of rs, anti-rs, and promoters.** *Mol Syst Biol* 2013, **9**:702.

720 **TABLE**

721 Table 1.Failure modes and engineering solutions for the design and built of layered genetic circuits in
722 single (bacterial) cell.

| Device | Failure Mode | Engineering Solution | Fig / [Ref] |
|----------------|---|--|--------------------------------|
| Input switches | Genetic crosstalk: Input switch devices cross-talk with one another. | <ul style="list-style-type: none"> ▪ Check pairwise compatibility by placing GFP and RFP under the regulation of each input switch device ▪ Perform mutagenesis on promoter or DNA-binding protein to identify orthogonal pairs. | S4 Ref [28, 29, 31, 50] |

| | | | |
|-----------------------------------|--|---|-------------------|
| | | | |
| AND gate | <p>Stoichiometric mismatch: Amount of AND gate's transcription activators are disproportionately matched, resulting in "leaky" AND gate.</p> | <ul style="list-style-type: none"> Characterise the expression profile of input genetic switches with different RBS and input the resultant transfer function equations into a steady state AND gate computational model. Match AND gate sub-modules to obtain stoichiometric balance using this forward engineering approach. | S11 |
| | <p>DNA supercoiling: $\sigma 54$ AND gate promoter is turned on by the DNA supercoil effects of upstream $\sigma 54$ promoter</p> | <ul style="list-style-type: none"> Insulate $\sigma 54$ promoters using different plasmid vectors. | S5 |
| OR gate | <p>Stoichiometric mismatch: Outputs from input device I and II are disproportionately matched, resulting in skewed OR gate.</p> | <ul style="list-style-type: none"> Characterise the expression profile of input genetic switches with different RBS and input the resultant transfer function equations into a steady state OR gate computational model. Match OR gate sub-modules to obtain stoichiometric balance using this forward engineering approach. | S12,S13 |
| | <p>Transcription interference: Tandem promoter OR gate design fails due to downstream DNA sequence acting as a repressor to upstream promoter.</p> | <ul style="list-style-type: none"> Characterise different permutation of tandem promoter OR gate to identify the optimal genetic architecture. Separate OR gate promoters into distinct expression cassettes. | 3A,3C 3A,3C |
| Layering OR-NOT into NIMPLY gate | <p>Insufficient repression: Placing single repressor binding site downstream of inducible promoter cannot fully repress gene expression.</p> | <ul style="list-style-type: none"> Increase repression efficiency by introducing additional repressor binding sites to the NOT gate. Note that the introduction of extra repressor binding sites may also lead to extensive 5'UTR effects. Attenuate expression "leakiness" by using weaker RBS for the NOT gate | 4A,4C 4B |
| | <p>Translation interference: Placing repressor binding sites downstream of inducible promoter creates extensive 5'UTR structural effects.</p> | <ul style="list-style-type: none"> Perform mutagenesis to relieve RNA hairpin structures at selected sites. Use RNA processing tools to remove undesired 5'UTR sequences. | S6 Ref [5, 20] |
| Layering AND-OR-NOT into XOR gate | <p>Insufficient repression: Insufficient transcription repressors are generated by upstream genetic circuit to stop transcription elongation, level mismatch.</p> | <ul style="list-style-type: none"> Reduce repressors required in NOT gate by designing repressor binding sites such that it is immediately downstream of transcription start site. Increase production of repressor in the AND gate by expressing transcription repressors in high copy plasmid. | 5 2D,5 |
| | <p>Translation interference: Placing repressor binding sites downstream of OR gate tandem promoter creates extensive 5'UTR structural effects.</p> | <ul style="list-style-type: none"> Separate OR gate promoters into distinct expression cassettes. Use RNA processing tools to remove undesired 5'UTR sequences. | 5 Ref [5, 20] |